

Focusing and trapping of DNA molecules by head-on ac electrokinetic streaming through joint asymmetric polarization

Cite as: Biomicrofluidics 4, 034108 (2010); <https://doi.org/10.1063/1.3481468>

Submitted: 31 May 2010 . Accepted: 31 July 2010 . Published Online: 19 August 2010

Jung-Rong Du, and Hsien-Hung Wei



View Online



Export Citation

ARTICLES YOU MAY BE INTERESTED IN

[Long-range and superfast trapping of DNA molecules in an ac electrokinetic funnel](#)

Biomicrofluidics 2, 044103 (2008); <https://doi.org/10.1063/1.3037326>

[Numerical study of in situ preconcentration for rapid and sensitive nanoparticle detection](#)

Biomicrofluidics 4, 034106 (2010); <https://doi.org/10.1063/1.3467446>

[ac electro-osmotic micropump by asymmetric electrode polarization](#)

Journal of Applied Physics 103, 024907 (2008); <https://doi.org/10.1063/1.2832624>



Biophysics Reviews

Publishing should be **EASY**, not stressful

Find out how
we're different!



Focusing and trapping of DNA molecules by head-on ac electrokinetic streaming through joint asymmetric polarization

Jung-Rong Du and Hsien-Hung Wei^{a)}

Department of Chemical Engineering and Center for Micro/Nano Science and Technology, National Cheng Kung University, Tainan 701, Taiwan

(Received 31 May 2010; accepted 31 July 2010; published online 19 August 2010)

In this work, invoking joint asymmetric ac polarization using double half-quadrupole electrodes in a symmetric arrangement, we demonstrate a head-on ac electro-osmotic streaming capable of focusing and trapping DNA molecules efficiently. This is manifested by the observation that picomolar DNA molecules can be trapped into a large crosslike spot with at least an order of magnitude concentration enhancement within just half a minute. We identify that the phenomenon is a combined result of the formation of two prefocused DNA jets flowing toward each other, dipole-induced attraction between focused DNA molecules, and dielectrophoretic trap on the spot. With an additional horizontal pumping, we observe that the trap can transform into a peculiar pitchfork streaming capable of continuous collection and long-distance transport of concentrated DNA molecules. We also show that the same electrode design can be used to direct assembly of submicrometer particles. This newly designed microfluidic platform not only has potentials in enhancing detection sensitivity and facilitating functional assembly for on-chip analysis but also provides an added advantage of transporting target molecules in a focused and continuous manner. © 2010 American Institute of Physics. [doi:10.1063/1.3481468]

I. INTRODUCTION

Detection and sensing of biomolecules not only are used to quantify contents of biological samples but also serve necessary means for medical diagnosis and sample fractionation. Since sample volumes are typically of nanoliters or smaller and concentrations of target molecules are of picomolar or lower, a successful operation often hinges on if the device has an ability to capture these molecules efficiently for enhancing the detection sensitivity with increased signals. Recent developments in micro-/nanotechnologies did offer renewed strategies for achieving this goal by trapping or preconcentrating dilute samples in micro-/nanodevices. Because most biomolecules are charged, it is tempting to enrich them under actions of applied electric fields. Along this line, a variety of techniques based on dc electrokinetics have been developed to concentrate analytes, including isoachophoresis,¹ isoelectric focusing,² field-amplified sample stacking,³ field-gradient focusing,⁴ electro-osmosis-assisted electrophoretic enrichment,⁵ and electrokinetic trap via concentration polarization across ion-selective filters or granules.^{6,7}

Recently, the use of ac electro-osmotic (ACEO) flow has become attractive to concentrate biomolecules under the theme of microfluidics.^{8–11} This flow arises from double layer polarization on electrodes under rapid charging and discharging by electric fields at frequencies of kilohertz or higher. Specifically, it is driven by oppositely acting Maxwell stresses within the double layers on polarized electrodes and emerges as a pair of counter-rotating vortices set up by the nonlinear time-averaged Smoluchowski slip velocity on the electrode surfaces,¹²

^{a)} Author to whom correspondence should be addressed. Electronic mail: hhwei@mail.ncku.edu.tw.

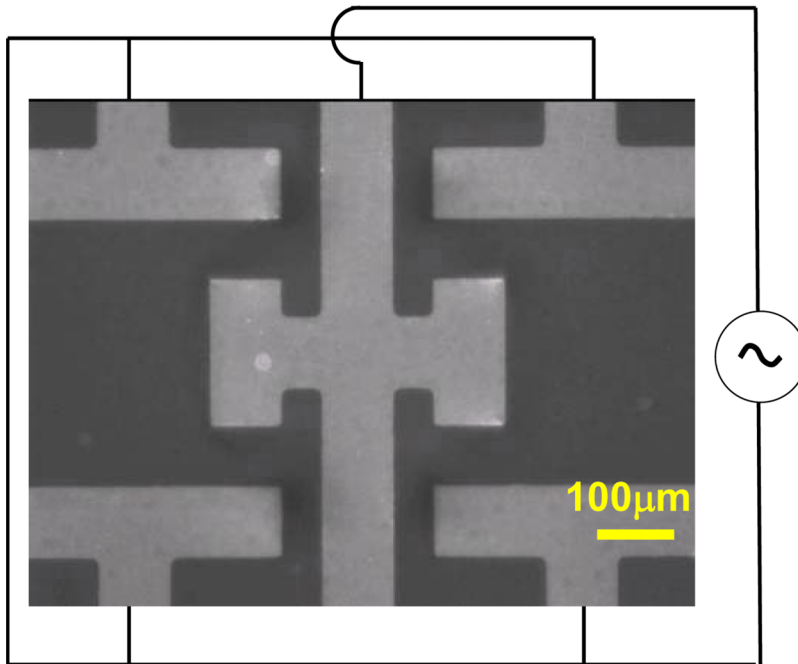


FIG. 1. Featured electrode system comprising two identical half-quadrupole electrode sets in a symmetric arrangement.

$$U_{\text{ACEO}} = -\frac{\varepsilon}{\eta} \langle \zeta(E_{\perp}) E_{\parallel} \rangle, \quad (1)$$

where ζ is the induced surface zeta potential that varies linearly with the normal field E_{\perp} on the electrodes, E_{\parallel} is the tangential field, and ε and η stand for the permittivity and viscosity of the sample solution, respectively. In contrast to the conventional dc approach, the use of ACEO in microfluidic applications has the following advantages. First, because of the quadratic dependence on electric field, the flow can be amplified more efficiently with electric field. Second, with suitable electrode designs, one can redirect flow toward specific sites or rectify streams into desired patterns.^{13–15} Lastly and more importantly, this flow can be incorporated with other ac effects such as dielectrophoresis (DEP) to facilitate trapping or assembly of colloidal particles and macromolecules.^{8,10,16–18}

In this work, we design a new electrode geometry to generate a structured ACEO for realizing efficient trapping of DNA molecules at the picomolar level. This paper is organized as follows. In Sec. II, we present our double quadrupole electrode design and present the ideas behind it. Experimental procedures are also provided in this section. The observed trapping phenomenon and quantification of concentration enrichment will be reported in Sec. III. The mechanisms underlying the trapping will be discussed in Sec. IV. In Sec. V, we demonstrate, with an additional pumping, that the trapping can transform into a pitchfork streaming for continuous collection and ejection of DNA molecules. We also set forth to apply the designed electrode system for directing assembly of submicrometer particles in Sec. VI. This paper is concluded in Sec. VII.

II. FEATURED ELECTRODE DESIGN AND EXPERIMENTAL PROCEDURES

The featured microelectrode design consists of two identical half-quadrupole electrode sets in a symmetric arrangement (see Fig. 1). Each electrode set comprises three T-shaped electrodes: two larger ones are faced to each other and the remaining one is placed on the side connected to the central vertical electrode. This design is intended to produce directional pumping through the asymmetric configuration in each half-quadrupole electrode set, but to generate a head-on focusing by combining the two through the global symmetry. To better visualize the movement of DNA

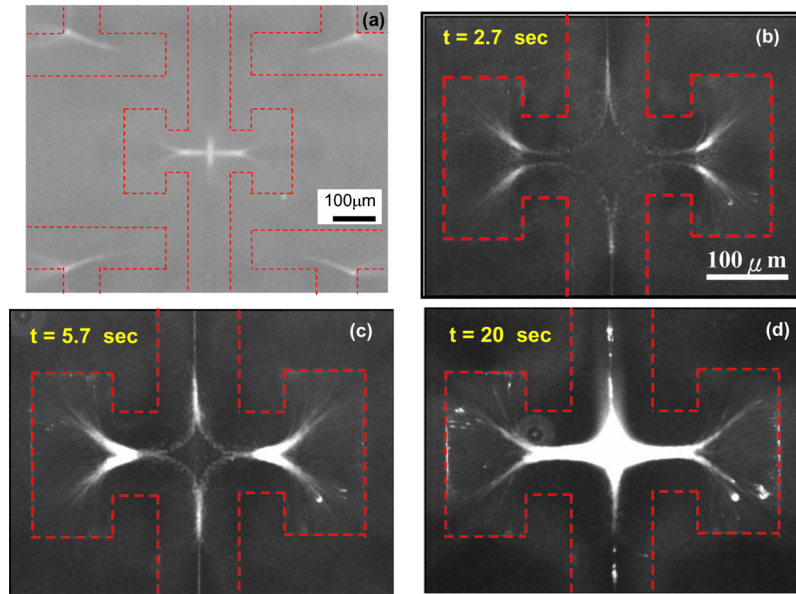


FIG. 2. (a) Observed DNA focusing and trapping in 1 $\mu\text{g}/\text{ml}$ DNA solution at 20 $V_{\text{p.p.}}$ and 1 kHz. (b)–(d) are snapshots showing head-on focusing of DNA streams.

molecules above the electrodes using an inverted microscope, the electrode system was made on a conducting, transparent indium tin oxide (ITO) glass substrate using standard photolithography techniques followed by wet etching. It was then housed in a 4.5 cm long polydimethylsiloxane microchannel of 120 μm in depth and 2000 μm in width. We used T4 DNA molecules (Wako, $MW=1.076 \times 10^8$) as our target molecules. They were intercalated with YOYO-1 fluorescent dyes every five basepairs. Various T4 DNA solutions were prepared at concentration from 10^{-3} $\mu\text{g}/\text{ml}$ (10^{-2} pM) to 1 $\mu\text{g}/\text{ml}$ (10 pM) in 1 mM tris-HCl buffer with 1% beta-mercaptoethanol. The conductivities of these DNA solutions were about 150 $\mu\text{S}/\text{cm}$ with the corresponding double layer thickness $\lambda=10$ nm. The use of such a high conductivity solution could make the system more vulnerable to Faradaic erosion. Yet, because an applied field actually flips its polarity very rapidly during a cycle, there would be insufficient time for Faradic charging unless frequency is excessively low. Hence, the system can be safely operated at voltages even beyond the Faradaic threshold.

After filling the desired DNA solution into the microchannel with a syringe pump (Cole Parmer), an electric field was then applied at voltage of 5–20 $V_{\text{p.p.}}$ (peak-to-peak voltage) using a function generator (Agilent 33220A). The frequency was chosen around the characteristic RC frequency $D/(\lambda L) \sim 1$ kHz at which Ohmic charging prevails,¹² where $L \sim 100$ μm is the width of the electrodes or the electrode separation and $D \sim 10^{-5}$ cm^2/s is the ionic diffusivity. The motion of DNAs was observed using an inverted fluorescence microscope (TE2000-S, Nikon) equipped with a cooled intensified charged coupled device (CCD) camera (CoolSNAP HQ², Roper Scientific). The fluorescence intensity was measured in real time with an image processing software (*in vivo*).

III. OBSERVED DNA TRAPPING AND CONCENTRATION ENHANCEMENT

After an application of 20 $V_{\text{p.p.}}$, DNA molecules are soon trapped into a bright, cross-shaped spot of about 200 μm in length at the midpoint of the central vertical electrode, as shown in Fig. 2(a). Snapshots in Figs. 2(b)–2(d) further reveal that this trapping is primarily driven by head-on ACEO jets merged from convergent streams coming from the corners of the sided electrodes, together with the additional assist by lining along the central vertical electrode.

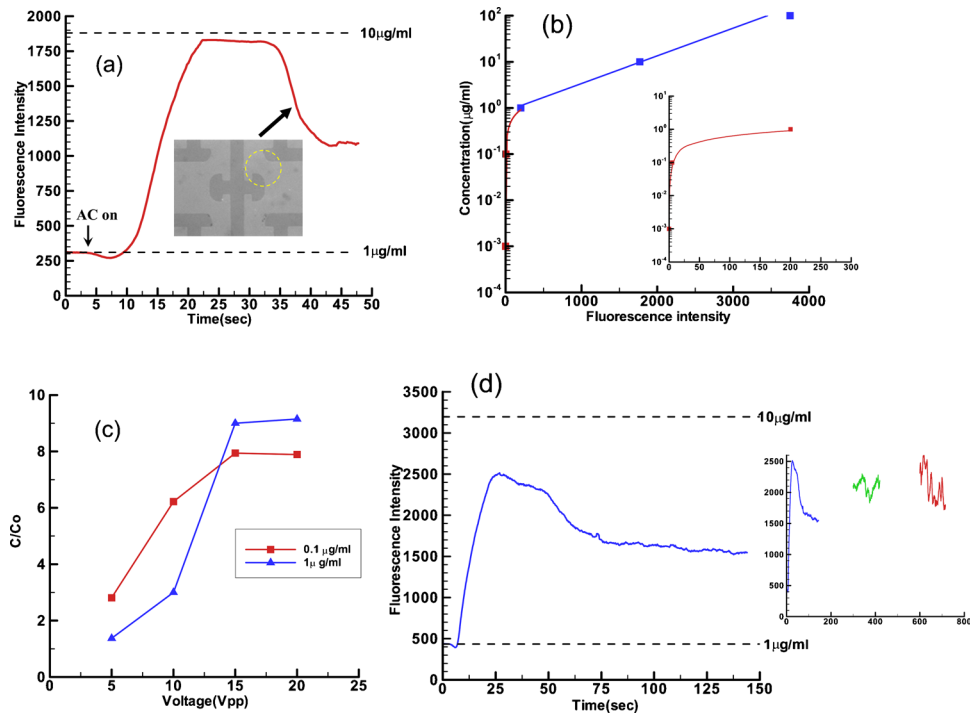


FIG. 3. (a) Measured fluorescence intensity as a function of time for concentrating 1 $\mu\text{g/ml}$ DNA solution at 20 $V_{\text{p.p.}}$ and 1 kHz. The inset reveals that there appears Faradaic erosion on the corner portions of the quadrupole electrodes, explaining the sharp decline in the fluorescence intensity after the maximum. (b) Measured relation between the DNA concentration and fluorescence intensity. (c) Measured concentration enrichment factor as a function of applied voltage for concentrating 0.1 and 1 $\mu\text{g/ml}$ DNA solutions. Distinct trapping responses of these solutions imply that part of the trapping mechanisms would have to involve intermolecular interactions between DNAs. (d) The same plot as (a) when gold electrodes are used. Compared to (a), the similar maximum can still be found but the fluorescent signal can last as long as 150 s during a detection, despite a postfading after the maximum due to photobleaching. Successive detections for every few minutes reveal that the maximum can be recovered repetitively. So the trapping actually persists for as long as 10 min as a result of a constant replenishment of fresh, unbleached DNA molecules.

Figure 3(a) shows the corresponding temporal evolution of the measured fluorescence intensity at the center of the focused DNA spot. To quantify the concentration enhancement, a calibration between the fluorescence intensity and DNA concentration is also carried out [see Fig. 3(b)]. As revealed in Fig. 3(a), after an application of 20 $V_{\text{p.p.}}$, it takes about 5 s to see a sharp rise in the fluorescent signal due to the local buildup of DNA molecules at the spot. This also means that it takes about the same amount of time for the flow to bring DNA molecules to the center of the central electrode at a speed of about 40 $\mu\text{m/s}$, as is revealed in Fig. 2(b). At about 15 s after turning on the field, the DNA concentration in the spot reaches a maximum. This maximum trap lasts for 15 s until a rapid decline in the fluorescence intensity appears. After the decline, the fluorescence intensity can still be maintained at about 60% of the maximum intensity, suggesting that the trapping is still at work but becomes somewhat sluggish, which will be explained later. By comparing the maximum fluorescence intensity of the trapped spot to the bulk value, we find that the DNA concentration is increased by about a factor of 10. The actual concentration enhancement could be even higher since the fluorescent dyes could become less emissive due to their self-quenching in a concentrated DNA environment.

Using C/C_0 , the ratio of the DNA concentration at the spot to the bulk value, to measure concentration enrichment, we plot this ratio as a function of applied voltage in Fig. 3(c) to quantify the trapping performance. At $C_0=1 \mu\text{g/ml}$, we find that C quickly rises to 9 times C_0 when increasing voltage from 5 to 15 $V_{\text{p.p.}}$. As the concentration increment here is roughly proportional to the square of voltage and so is ACEO, this suggests that the trapping is primarily determined by

convective ACEO focusing. At voltages higher than $15 V_{p.p.}$, however, the DNA concentration in the spot ceases to grow and reaches a plateau. This implies that the spot cannot accommodate more DNAs by rising voltage and hence the ability to further build up DNAs becomes saturated. At $C_0=0.1 \mu\text{g/ml}$, the concentration enrichment is found to be higher than that at $C_0=1 \mu\text{g/ml}$ in the voltage range of $5-15 V_{p.p.}$, whereas the plateau value is lower. In addition, the observed concentration rise roughly varies linearly with voltage, which is slower than the quadratic rise found at $C_0=1 \mu\text{g/ml}$. For a very dilute DNA solution such as $C_0=10^{-3} \mu\text{g/ml}$, however, we do not observe any discernable increase in the fluorescent signal in the same range of voltage. These distinct trapping responses at different bulk concentrations suggest that the trapping is not solely determined by convective ACEO focusing; part of the trapping mechanisms must involve intermolecular interactions between DNAs and such interactions have to be field-dependent, as will be discussed later in Sec. IV B.

Now returning to the sharp decline in the fluorescence intensity after the maximum shown in Fig. 3(a), we identify that it is not due to photobleaching of the fluorescent dyes, but simply to the loss of the trapping power by Faradaic erosion on the quadrupole electrodes [see the inset in Fig. 3(a)]. Such erosion, though Ohmic charging predominates here, can still occur locally at places such as sharp electrode corners where current densities are high, to which ITO electrodes seem more susceptible because of its relative low Faradaic threshold voltage. This problem can be eliminated by using gold electrodes (beneath which there is a chromium layer for aiding in adhesion). By monitoring the fluorescence intensity every few minutes, the maximum intensity can be detected repetitively, despite a slight postfading of the fluorescent signal due to photobleaching during detection [see Fig. 3(d)]. This observation suggests that the trapping indeed persists without being disrupted by Faradaic reactions (if they exist). In fact, the trapping can actually be maintained for more than 10 min, as seen in Fig. 3(d). Since photobleaching is typically an irreversible process, the observed reappearance of the maximum intensity during successive detections could be attributed to a constant replenishment of fresh, unbleached DNA molecules into the focused spot.

We also examine the effects of frequency on the trapping. We find that if frequency is far different from the RC frequency, the trapping will not occur due to the lack of formation of the head-on ACEO focusing, which will be explained in more detail in Sec. IV A.

IV. PHYSICAL MECHANISMS RESPONSIBLE FOR THE OBSERVED DNA TRAPPING

We surmise that the observed DNA trapping is a combined result of three mechanisms: (i) focusing of DNA molecules by head-on ACEO streaming, (ii) dipole-induced self-attraction between focused DNA molecules, and (iii) dielectrophoretic trap of the focused spot. Figure 4 gives an overview of how DNA molecules are focused and trapped due to these mechanisms. Below we provide detailed accounts for each mechanism.

A. Focusing of DNA molecules by head-on ACEO streaming

As in Ref. 12, we start with the basic mechanism of ACEO due to Ohmic charging by a pair of symmetric coplanar electrodes [see Fig. 5(a)]. Now imagine what happens during an arbitrary half cycle of an applied ac field. For the anode on the left, negatively charged counterions are induced within the double layer on the electrode surface. The electric field emitting from there therefore imparts a Coulombic force toward the left on these induced charges. Similarly, for the cathode on the right on which positive charged counterions are induced, the resulting Coulombic force is toward the right over the electrode surface. These two oppositely acting forces thus in turn drive the fluid outward along the electrode surfaces, creating a symmetric pair of counter-rotating vortices with a divergent stagnation point in between the electrodes. If the electrodes are not equal in size, the resulting vortex structure becomes asymmetric with vortices of different sizes and intensities. The stronger vortex on the smaller electrode is rolling faster than the weaker one on the larger electrode, redirecting a net flow from the former to the latter,¹³ as delineated in Fig. 5(b).

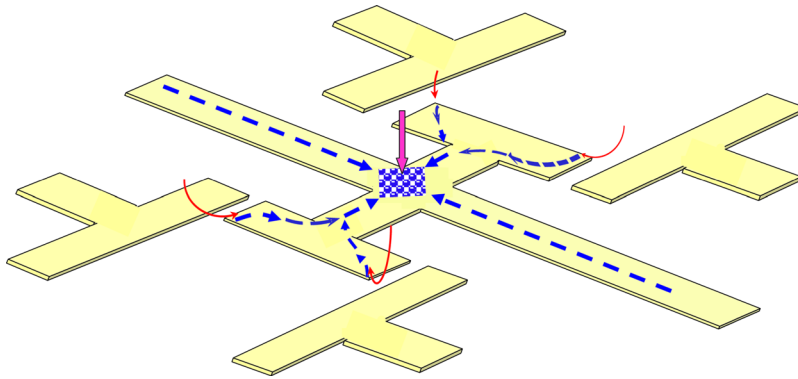


FIG. 4. Schematic illustration of how DNA molecules undergo focusing and trapping. DNA molecules (indicated by blue) are first prefocused by converging streams generated by ACEO vortices (marked by red) from the corners of the sided T-shaped electrodes. The two prefocused DNA streams then undergo head-on collision to trap DNAs at the center of the system, with the additional assistance of dipole-induced association between focused DNAs and the holding of the trapped spot by the downward DEP force (indicated by a pink arrow).

With Fig. 5(b) in mind, the ACEO funnel and hence the subsequent formation of a focused DNA jet in each half-quadrupole electrode set can be readily explained, as shown in Fig. 6. Since the length of the smaller T-shaped electrode is greater than the width of the two larger electrodes in the orthogonal arrangement, a net pumping must occur from the former to the latter due essentially to the mechanism shown in Fig. 5(b). Specifically, this orthogonal electrode arrangement forms tilted ACEO vortices in which more intense vortex occurs on the smaller T-shaped electrode side. As a result, the fluid will be drained from the two larger T-shaped electrodes and then focused toward the smaller T-shaped electrode. This draining effect in turn gives rise to two oblique focused ACEO streams from the corners toward the middle of the T-shaped electrode. Upon merging of these two streams, a funnel will then form to collect DNA molecules toward the converging stagnation point where the streams meet. Subsequently, a focused DNA jet will emerge and be heading toward the central vertical electrode. Since there is also a focused DNA jet coming from the other side of the central vertical electrode, these two jets will be moving toward each other, creating the observed head-on ACEO streams for focusing DNA molecules.

It is worth remarking that the observed trapping can only be realized around the RC frequency so that the head-on ACEO can be maximized due to the Ohmic charging. This can be seen more clearly from how the ACEO velocity varies with frequency,¹²

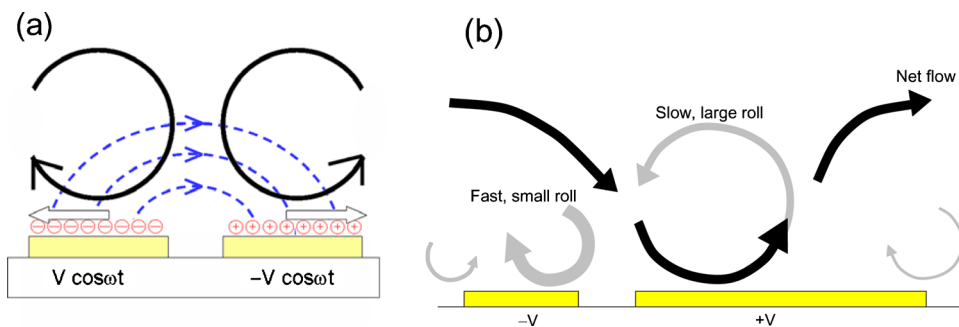


FIG. 5. Mechanisms of ACEO vortices and pumping. (a) shows how ACEO vortices (in black) are generated by Ohmic charging on coplanar electrodes. Electric field lines are indicated by blue. Arrows on the electrode surfaces indicate the directions of the induced Coulomb forces within the double layers. (b) illustrates how a net fluid pumping is generated by asymmetric ACEO vortices when the electrodes are of unequal sizes.

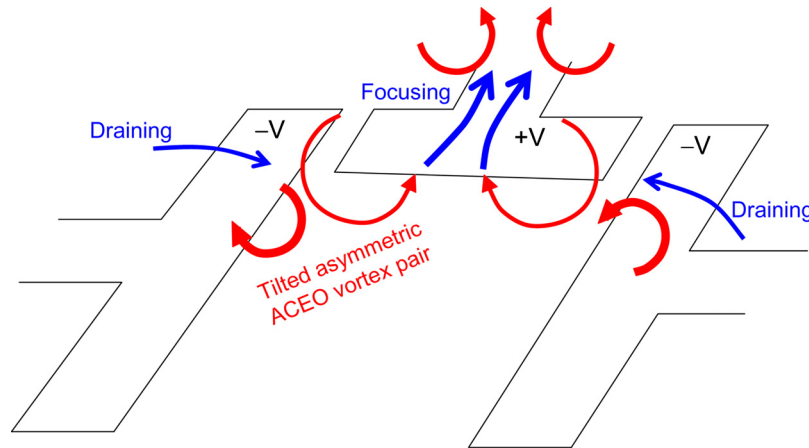


FIG. 6. Schematic mechanism for the formation of ACEO funnel generated by the half-quadrupole electrode set. Because of the asymmetric electrode configuration, asymmetric polarization on the adjacent, orthogonal electrodes will create tilted ACEO rolls in which more intense microvortices take place along the edges of the larger T-shaped electrodes, producing two converging streams to drain the fluid toward the smaller T-shaped electrode in between. These two streams then soon merge into a funnel, collecting the surrounding DNA molecules to form a prefocused jet moving toward the central vertical electrode.

$$U_{\text{ACEO}} \sim \frac{\Omega^2}{(1 + \Omega^2)^2} \frac{\epsilon V^2}{\eta L}, \quad (2)$$

where $\Omega = \omega/(D/\lambda L)$ is the dimensionless frequency normalized by the RC frequency $D/\lambda L$. Equation (2) indicates that U has a maximum at $\Omega = 1$. The existence of the optimal frequency for ACEO can be understood as follows. If frequency is too high, there will be insufficient time to produce enough counterions on the electrode surface. On the other hand, at too low frequency the surface field will be screened by abundant counterions. Either case will make ACEO more sluggish. Note that if frequency is excessively low, there will be Faradaic charging that can build up coions instead to reverse the flow direction. In this case, the resulting flow around the center point will become diverging and hence will not be able to focus and trap DNA molecules.

B. Field-induced attraction between polarized DNA molecules

The observed DNA trapping, however, cannot be sustained alone by convective ACEO focusing, as whatever is injected by the flow must be ejected for fulfilling the requirement of fluid mass conservation. In addition, the trapping is inevitably opposed by molecular diffusion that tends to disperse focused DNA molecules back to the bulk. Hence, additional mechanisms must be at play to against these adverse effects. Aside from the natural van der Waals attraction, one plausible mechanism that can keep DNA molecules from dissociation when they are focused is field-induced dipole-dipole attraction. As illustrated in Fig. 7, this mechanism is rooted in polarization of DNA molecules induced by an applied electric field so that two polarized DNA coils can be bound through attraction between neighboring induced dipole charges of oppositely signs, resembling chaining of polarized particles in an electric field.¹⁹

To see how such dipolar attraction occurs, we consider DNA molecules (of the radius of gyration R) subjected to an electric field E . The induced dipole moment is given by

$$\mu = 4\pi\epsilon R^3 KE, \quad (3)$$

where K is the polarizability measured by the real part of the Clausius–Mossotti factor. For two interacting polarized DNA molecules of separation r , it can be shown that the interaction energy is $-\mu^2/2\pi\epsilon r^3$.²⁰ With the aid of Eq. (3), this energy reads as

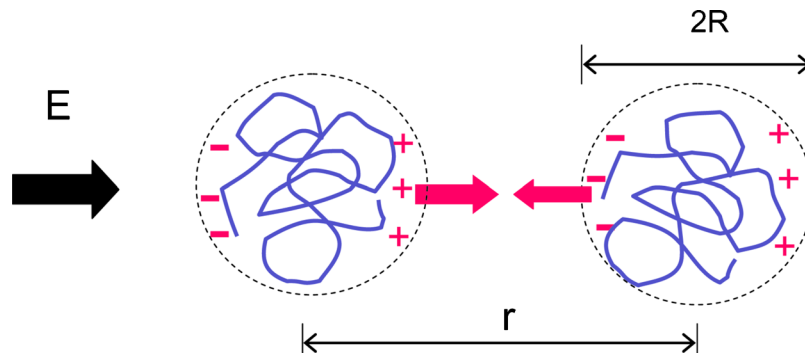


FIG. 7. Schematic illustration of field-induced self association between two polarized DNA coils (in blue). The association is caused by the attraction between the neighboring dipole charges of oppositely signs.

$$\psi_{dd} = -8\pi\epsilon R^3 \phi K^2 E^2, \quad (4)$$

where $\phi = (R/r)^3$ is the volume fraction of DNA. Such field-induced attraction between polarized DNA molecules can only occur if ψ_{dd} exceeds the thermal energy $k_B T$ in magnitude to prevent disruption by thermal fluctuations. With $\phi \sim 10^{-4}$ in $0.1 \mu\text{g/ml}$ DNA solution and $E \sim 10^3 \text{ V/cm}$ used in the experiment, we find that the ratio $|\psi_{dd}|/k_B T$ is an order of 10^2 , indicating that DNAs can indeed be tightly held by an electric field upon being focused. However, for a very dilute DNA solution such as $10^{-3} \mu\text{g/ml}$, $|\psi_{dd}|/k_B T$ is merely an order of unity. This means that the dipolar energy is comparable to the thermal energy, but not strong enough to hold DNAs against diffusion. This explains why we are not able to observe appreciable trapping in this case.

C. Dielectrophoretic trap on the focused spot

With the aid of the dipolar attraction above, focused DNAs can form an aggregate, allowing a steady buildup of DNA molecules at the converging stagnation point through the injection by the head-on ACEO streaming. When this aggregate grows into a larger clump like a spot, say, of size a , DEP would join to hold the spot against the upward sweeping created by the head-on ACEO injection, as illustrated by Fig. 8. Such a DEP-assisted trapping mechanism has been suggested to explain the observed particle trapping by ACEO vortices,^{8,10,17} and demonstrated in the recent theoretical study.¹⁸

The DEP force can be described by²¹

$$F_{\text{DEP}} = 2\pi\epsilon a^3 K \nabla |E|^2. \quad (5)$$

This DEP trap on the spot can only be realized when positive DEP (i.e., $K > 0$) occurs to attract the spot toward the electrode surface near which fields are high. Balancing $F_{\text{DEP}} \sim 2\pi a^3 \epsilon V^2/d^3$ with

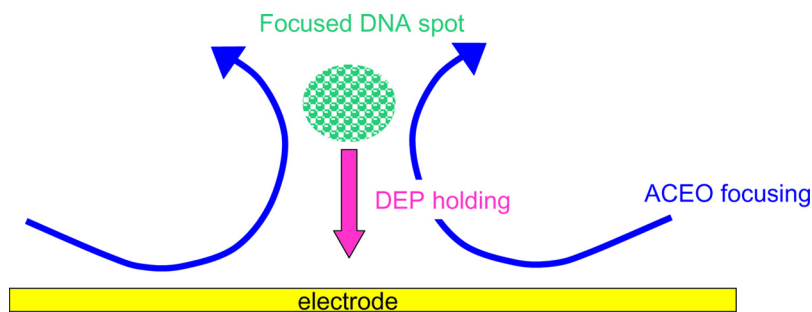


FIG. 8. Schematic illustration of how a focused DNA spot is held by a downward DEP force against the upward flow by the ACEO focusing.

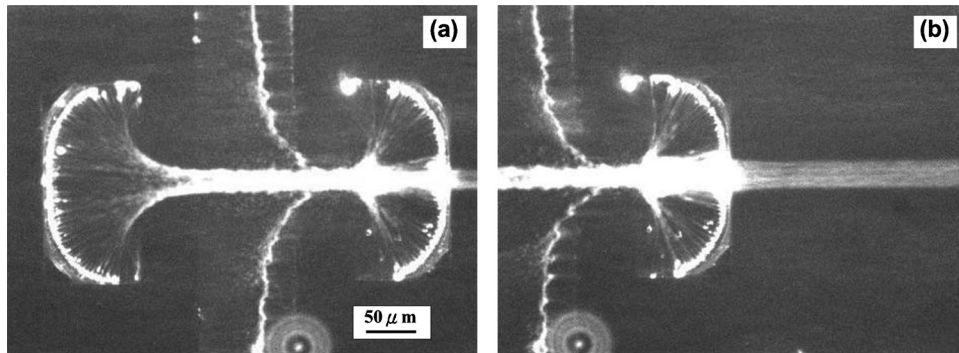


FIG. 9. Formation of pitchfork streaming by first carrying out the trapping of 1 $\mu\text{g/ml}$ DNA at 20 $V_{\text{p.p.}}$ and 1 kHz and then applying an additional horizontal pumping of 0.5 ml/h toward the right while keeping the ac field on. A steady ejection of a concentrated DNA jet is observed due to continuous collection of DNA from split streams toward the converging point at the right.

the drag force $F_{\text{ACEO}} \sim 6\pi\eta a U_{\text{ACEO}} \sim 6\pi\epsilon a V^2/L$, we find that the spot size scales as $a \sim (3d^3/L)^{1/2}$, where d ($\sim 100 \mu\text{m}$) is the distance of the spot to the electrode surface and L ($\sim 100 \mu\text{m}$) is the electrode dimension. Hence, the estimated spot size is about 170 μm , which agrees with what we see in Fig. 2(d).

It is worth pointing out that both dipolar attraction and DEP holding mentioned above are typically short-range. These effects manifest mostly when DNAs come close to the electrode surface or near each other. Because the ACEO focusing here acts to assist in packing DNAs and these two short-range effects work to resist depletion by the flow, this explains why the trapped DNA spot can still be maintained during the focusing. In other words, DNAs are first brought distantly from the bulk to form a compact spot by the ACEO focusing, and then immediately undergo short-range self-association and DEP due to induced dipoles, resulting in the fast DNA trapping phenomenon observed in the experiment.

Nonetheless, there are several aspects worth mentioning concerning how to optimize the trapping with a proper electrode design. First, it might appear that the most efficient way to enhance the trapping is amplifying electric fields by decreasing the electrode separation/size. However, the Faradaic erosion, especially on sharp electrode corners, could become more likely to occur to diminish the trapping efficiency. This problem can be relieved by lowering local electric fields via making these corners rounded. In this way, the overall field strength can still be elevated using smaller electrodes without suffering the Faradaic erosion. Also because a higher ac frequency must be chosen for optimizing the charging with the shorter RC time, this provides an additional help for reducing Faradaic currents. Second, for each quadrupole electrode set, we only take half the quadrupole configuration without including the outer side electrode. This asymmetric electrode design is to assure that most of the draining power can be directed to drive DNAs toward the central electrode without being split by the outward flow generated by the outer side electrode. Lastly, there is an additional ACEO streaming generated by the orthogonal arrangement of the central vertical electrode and the horizontal parts of the quadrupole electrodes. This flow could draw DNAs away from the focused spot and hence could lower the trapping efficiency. Such an effect could be minimized by either shortening the width of the central electrode or increasing its separation to the adjacent horizontal electrodes.

V. CONTINUOUS DNA COLLECTION AND EJECTION BY PITCHFORK STREAMING

We further demonstrate that trapped DNA molecules can be conveyed by a continuous flow to form a concentrated DNA stream. As shown in Fig. 9, with an additional horizontal pumping of 0.5 ml/h while keeping the ac field on after the trapping by the ACEO, we observe a pitchfork streaming resulted from merging of split DNA streams into an emanating DNA jet, showing continuous collection and ejection of DNA molecules. The speed of the pumping is about

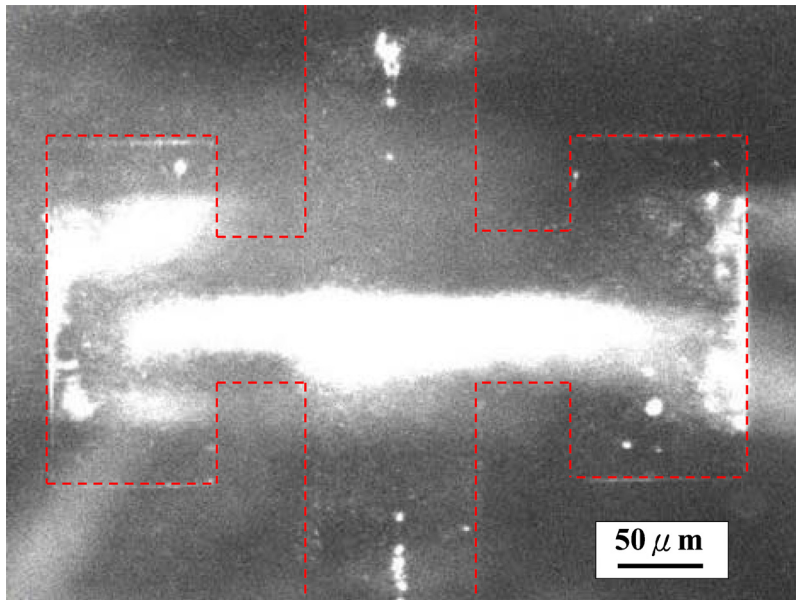


FIG. 10. Transport of trapped DNA molecules toward the right by applying a dc field of 40 V/cm toward the left after the ac trap at 20 V_{p,p} and 1 kHz in 1 μg/ml DNA solution. Here we use gold electrodes to carry out the experiment to prevent possible electrode erosion arising from dc Faradaic charging.

580 μm/s, which is much faster than the observed ACEO velocity (<100 μm/s). As the trapping can still be sustained in such a fast sweeping without being destroyed, we speculate that not only are the trapped DNA molecules held strongly by DEP against the sweeping, but also the trapping actually occurs near/on the electrode surface where the actual sweeping would be diminished by the much slower fluid velocity thereof.

Aside from pumping, we have also applied a dc field (in the horizontal direction) after the trapping to transport as-trapped DNA molecules electrophoretically. However the result appears not as efficient as that with an additional pumping due perhaps to the lack of convective focusing to suppress lateral dispersion of DNA molecules (see Fig. 10). Early studies^{8,11} have shown that the addition of a dc bias to an ac signal can enhance DNA trapping onto electrode surfaces. We expect that the similar approach might help the collection of trapped DNA molecules using our electrode design.

VI. DIRECTED ASSEMBLY OF SUBMICROMETER PARTICLES

In addition to trapping DNA molecules, we employ the same electrode design for directing assembly of submicrometer colloids. In the experiments, latex particles of 6 μl (density = 1.05 g/ml, Duke Scientific) were suspended in the same 1 ml buffer solution used in the DNA trapping experiment. Two different particle sizes, 0.1 and 0.92 μm in diameter, were also employed to see how effects of particle size play roles. The experiments were carried out at 20 V_{p,p} with three different frequencies: 1 kHz, 100 kHz, and 20 MHz.

Figure 11 shows the observed particle aggregation behaviors. For 0.1 μm particles, at 1 kHz they are trapped into a bright compact cross, similar to Fig. 2(d) when trapping DNA. At a higher frequency 100 kHz, a similar trapping pattern is still observed but appears less compact compared to that at 1 kHz. When going to an even higher frequency 20 MHz, no apparent particle aggregation can be seen. The resemblance of the observed particle assembly to the trapped DNA pattern and its diminishing by increasing frequency away from the system's RC frequency 1 kHz suggest that the assembly is mainly directed by ACEO. In fact, we have observed that some of these particles are constantly recirculating above the electrode—the signature of ACEO vortices. As for larger, 0.92 μm particles, their trapping patterns at 1 and 100 kHz are not as apparent as those of

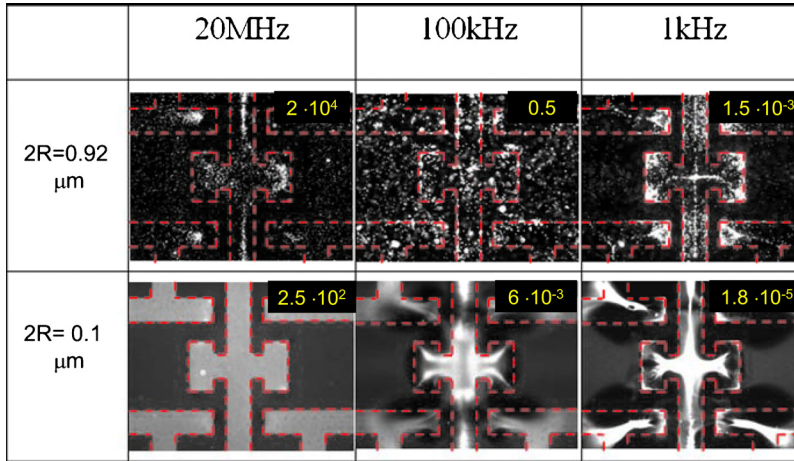


FIG. 11. Trapping of submicrometer particles at 20 V_{p,p} and distinct behaviors are found when different ac frequencies are applied. The experiments are carried out using gold electrodes. For 0.1 μm sized particles, at 1 kHz they are trapped by ACEO in a manner similar to that of DNA [Fig. 2(d)]. At 100 kHz, a similar trapping pattern is still observed but appears less compact, whereas no apparent trapping is found at 20 MHz. For larger, 0.92 μm sized particles, the observed trapping patterns at 1 and 100 kHz appear less apparent compared to those of 0.1 μm sized particles. At 20 MHz, particle aggregation is somewhat visible due to DEP that is more pronounced for larger particles. The number shown in the upper right corner of each panel is the DEP to ACEO velocity ratio to highlight the relative importance between DEP and ACEO.

0.1 μm particles. In fact, no obvious particle trapping is observed at 100 kHz. At 20 MHz, in contrast to the absence of assembly for 0.1 μm particles, the particles can assemble into a visible pattern, which cannot be attributed to ACEO but to DEP.

In short, at 1 kHz we see vivid crosslike particle assembly for the smaller particles and similar but less apparent aggregation for the larger particles. At 20 MHz, on the contrary, we do not observe any trapping for the smaller particles but do see for the larger particles. These frequency and size dependent particle aggregation behaviors can only be explained by distinct natures between ACEO and DEP: The particle motion at 1 kHz is dictated by ACEO which tends to trap smaller particles more effectively with less impacts from DEP, while DEP prevails at 20 MHz and is more pronounced for larger particles.

To further quantify if it is ACEO or DEP governing the particle motion, we take the ratio between their velocity scales to see how their relative importance varies with frequency and particle size. For a particle of radius R its DEP velocity scales as $U_{\text{DEP}} = F_{\text{DEP}} / 6\pi\eta R \sim \varepsilon R^2 K V^2 / \eta L^3$ according to Eq. (5). Its ratio to the ACEO velocity scale $U_{\text{ACEO}} \sim (\varepsilon V^2 / \eta L) \Omega^2 / (1 + \Omega^2)^2$ from Eq. (2) yields

$$\Gamma = \frac{U_{\text{DEP}}}{U_{\text{ACEO}}} \sim K \frac{R^2 (1 + \Omega^2)^2}{L^2 \Omega^2}, \quad (6)$$

with $\Omega = \omega / (D/\lambda L)$. Here the particle's polarizability K ranges from -0.5 (as $\omega \rightarrow \infty$) to 0.5 (as $\omega \rightarrow 0$) and hence does not change its magnitude as ω varies. Equation (6) reveals that if ω is not too far from the RC frequency $D/\lambda L$, ACEO outweighs DEP and the smaller particles, the more important ACEO is. However, DEP can rise against ACEO as ω is increased beyond $D/\lambda L$. At an excessively high ω , DEP could dominate over ACEO if the particle sizes were large enough to cause $\Gamma \sim (R/L)^2 \Omega^2 > 1$ in Eq. (6).

As such, with the aid of Eq. (6), results shown in Fig. 11 can be readily understood. At 1 kHz, ACEO dominates the trapping because Γ is very small for either particle suspension. The crosslike trapping of 0.92 μm particles is less apparent because it is opposed by DEP with the larger Γ . In fact, it could be positive DEP that tends to defocus the particles by attracting some of them toward the electrode corners (see the result of 0.92 μm particles at 1 kHz). At 100 kHz, 0.1 μm particles still show a crosslike trapping by ACEO with a very small Γ . For 0.92 μm particles, however,

there is no apparent particle aggregation since ACEO and DEP oppose each other in a similar magnitude. At 20 MHz, it is obvious that DEP is responsible for the observed trapping of 0.92 μm particles in view of a very large Γ . Note that the trapping here seems to occur inside the electrodes (instead of around the electrode corners at 1 kHz) and part of it takes place along the central vertical line of the central electrode. This is due perhaps to negative DEP that tends to trap particles toward places where electric fields are low. Although DEP appears dominant over ACEO for 0.1 μm particles, nothing happened virtually to these particles. This is because the estimated particle DEP velocity $U_{\text{DEP}} \sim 10^{-1}$ $\mu\text{m/s}$ is too low to make the trapping occur. Specifically, a DEP trap can only be realized when the time scale required to trap particles, L/U_{DEP} , is much shorter than the particle diffusion time L^2/D_p so that trapped particles will not have time to diffuse back, where $D_p = k_B T / 6\pi\eta R$ is the particle diffusivity with $k_B T$ being the thermal energy. However in this case $L/U_{\text{DEP}} \sim 10^3$ s is comparable to L^2/D_p and hence cannot make DEP at work.

VII. CONCLUDING REMARKS

We have demonstrated efficient focusing and trapping of DNA molecules with head-on ACEO streaming generated by double half-quadrupole electrode design. In contrast to the simple eccentric electrode design in early studies,^{8,9,11} we invoke a new design concept: join asymmetric polarization, which involves an asymmetric electrode configuration in a symmetric arrangement, to realize the trapping. We show that this design is capable of trapping picomolar DNA molecules into a large concentrated spot with at least an order of magnitude concentration enhancement within just half a minute. We also identify that the trapping is a process collaborating several mechanisms: convective focusing by the head-on ACEO streams, dipole-induced self-association between focused DNAs, and DEP trap on the focused spot. In addition, we show, with an additional horizontal pumping, that the ACEO trap can transform into a pitchfork streaming capable of continuous collection and long-distance transport of DNA molecules, which has not been seen by any of prior studies. What is more, our platform is not limited to trapping DNA. We demonstrate the use of the same electrode design in directing assembly of submicrometer particles.

As such, our platform cannot only be used in preconcentration of dilute samples for enhancing detection sensitivity but can also be applied to manipulate colloidal particles for forming desired patterns. It might also provide a new route to facilitate hybridization of target biomolecules for molecular assay, which will be explored in our future study.

ACKNOWLEDGMENTS

This work was supported by the National Science Council of Taiwan under Grant No. NSC 97-2628-E-006-001-MY3 of H.-H.W.

¹P. A. Walker, M. D. Morri, M. A. Burns, and B. N. Johnson, *Anal. Chem.* **70**, 3766 (1998).

²P. G. Righetti and A. Bossi, *Anal. Chim. Acta* **372**, 1 (1998).

³B. Jung, R. Bharadwaj, and J. G. Santiago, *Electrophoresis* **24**, 3476 (2003).

⁴D. N. Petsev, G. P. Lopez, C. F. Ivory, and S. S. Sibtett, *Lab Chip* **5**, 587 (2005).

⁵J. Dai, T. Ito, L. Sun, and R. M. Crooks, *J. Am. Chem. Soc.* **125**, 13026 (2003).

⁶Y. C. Wang, A. L. Stevens, and J. Han, *Anal. Chem.* **77**, 4293 (2005).

⁷S.-C. Wang, H.-H. Wei, H.-P. Chen, M.-H. Tsai, C.-C. Yu, and H.-C. Chang, *Biomicrofluidics* **2**, 014102 (2008).

⁸P. K. Wong, C.-Y. Chen, T.-H. Wang, and C.-M. Ho, *Anal. Chem.* **76**, 6908 (2004).

⁹M. R. Bown and C. D. Meinhart, *Microfluid. Nanofluid.* **2**, 513 (2006).

¹⁰J.-R. Du, Y.-J. Juang, J.-T. Wu, and H.-H. Wei, *Biomicrofluidics* **2**, 044103 (2008).

¹¹K. F. Lei, H. Cheng, K. T. Choy, and L. M. C. Chow, *Sens. Actuators, A* **156**, 381 (2009).

¹²N. G. Green, A. Ramos, A. Gonzalez, H. Morgan, and A. Castellanos, *Phys. Rev. E* **66**, 026305 (2002).

¹³A. Ramos, A. Gonzalez, A. Castellanos, N. G. Green, and H. Morgan, *Phys. Rev. E* **67**, 056302 (2003).

¹⁴D. Lastochkin, R. Zhou, P. Wang, Y. Ben, and H.-C. Chang, *J. Appl. Phys.* **96**, 1730 (2004).

¹⁵J.-T. Wu, J.-R. Du, Y.-J. Juang, and H.-H. Wei, *Appl. Phys. Lett.* **90**, 134103 (2007).

¹⁶N. G. Green, A. Ramos, and H. Morgan, *J. Phys. D: Appl. Phys.* **33**, 632 (2000).

¹⁷J. Wu, Y. Ben, D. Battigelli, and H.-C. Chang, *Ind. Eng. Chem. Res.* **44**, 2815 (2005).

¹⁸S.-J. Liu, S. H. Hwang, and H.-H. Wei, *Langmuir* **24**, 13776 (2008).

¹⁹S. Takashima and H. P. Schwan, *Biophys. J.* **47**, 513 (1985).

²⁰S. Fraden, A. J. Hurd, and R. B. Meyer, *Phys. Rev. Lett.* **63**, 2373 (1989).

²¹H. A. Pohl, *Dielectrophoresis* (Cambridge University Press, Cambridge, 1978).